Measuring performance of integrated air defense networks using stochastic networks

ARTICLES

MEASURING PERFORMANCE OF INTEGRATED AIR DEFENSE NETWORKS USING STOCHASTIC NETWORKS

MICHAEL P. BAILEY

Naval Postgraduate School, Monterey, California

(Received August 1989; revisons received January, October 1991; accepted December 1991)

A model reflecting the evolution of an engagement between an integrated air defense system (IADS) and a penetrating strike group is presented. The engagement is modeled as an optimization problem on a network with stochastic arc lengths. We produce the distribution of our measure of effectiveness, as well as calculating the importance of each IADS agent to the performance of the overall system. We demonstrate the effectiveness of several jamming plans against the network.

Since World War II, interest has been growing steadily in techniques which exploit the electromagnetic spectrum to gather intelligence in the support of warfare. Consequently, methods have been developed for preventing radars from being effective: electronic countermeasures (ECM). Aircraft and ground systems capable of using ECM techniques to jam air defense radar allow air strikes to be performed with greater safety to the attacking force.

A longstanding problem faced by those employing ECM is the evaluation of the degradation in the performance of the air defense system caused by jamming. In this paper, we propose to measure this performance as the time elapsed between the time a strike group enters a defended area and the time the air defense system fires upon the strike group. This time is the convolution of detection, data fusion, and decision task times.

Each of these task times is assumed to be a random variable. Furthermore, in the dense radar environment observable throughout most of the world, there are several emitters searching each cubic meter of airspace. These emitters are linked in a hierarchical communications network so they may share information and so command and control may be performed. Thus, the time required for an unalerted air defense network to prepare to fire a weapon can be seen to be the solution to a stochastic network optimization problem.

We will call our network model the *relaxed Petri model*. Special cases of this model include Petri nets, shortest paths, and PERT network models. In fact, the relationship of PERT networks, Petri nets, and relaxed Petri nets is hierarchical in terms of generality, with the hierarchical order given as listed. Kulkarni (1984), Kulkarni and Adlakha (1984), and Haas and Shedler (1988), respectively, study these network models when the arc lengths or task times are allowed to be random variables. The network of Levis (1986) was the first where any type of military data or command network was modeled using Petri nets, though this effort was limited to deterministic task times. This work was expanded by Remy (1986).

1. BACKGROUND

Most jammer planning by current tactical aircraft is done on a target-by-target basis. The director of an air strike is presented with a map which indicates the location and signal characteristics of each known air defense emitter near the strike target. The decision is made to jam a subset of the emitters in a prespecified sequence to increase the survivability of the air strike. This decision is constrained by the availability of jamming assets carried by the jamming aircraft. An emitter may be jammed only if the aircraft is carrying the jamming pod designed to match the emitter's signal characteristics. Furthermore, the pod must be

Subject classifications: Military: tactics and strategy. Probability: Markov processes and stochastic model applications.
Area of review: MILITARY.

0030-364X/92/4004-0647 $01.25

aimed at the target emitter to be effective. The aircraft is configurable to meet specific mission needs, but it can only carry a limited number of jamming pods.

The ECM targets in an air defense force are classified functionally as early warning, height finding, target acquisition, and target tracking. Several of each type of emitter are tied together with several non-emitting data fusion nodes and one or more command posts in a hierarchical network. When attacked, this network progresses through a series of engagement states, progressing from unalerted to higher states of engagement and threat awareness. The behavior of the IADS is described as the engagement takes place in Heilenday (1988). The description found there forms the basis for our model.

Consider the tactical situation diagrams in Figures 1–4. Each small circle represents emitter locations, while the attached larger circles are range rings. The heavy line represents a flight path of a strike group passing through this area. Also pictured are a data fusion center, an early warning (EW) report center, a zone command center, and two battalion command posts. At a data fusion node, data supplied by one or more early warning emitters are processed, the result being transmitted to height finding emitters in the area, and to the zone command node. At a zone command node, decisions are made about whether the air defense network will attack a target, and issue commands to that effect. For any weapon to be launched, the associated target tracking radar must be locked onto the target and the required command to fire must have been received from the zone command node.

In Figure 5, we show the evolution of an air defense system's state as it engages an intruder. The system starts the engagement when one of its EW emitters detects a possible threat. It transmits this information to the EW report center, which processes the detection data and issues a broadcast which is received by all target acquisition emitters, the data fusion node, and the zone command node.

The target acquisition emitters attempt to develop a two-dimensional solution of the incoming aircraft. They share their tracking data with a central target acquisition data fusion node. Height finding (HF) emitters are designed to determine the incoming aircraft's height. These emitters must have the two-dimensional target acquisition solution to search effectively for the intruder. Target trackers use the three-dimensional track to develop a solution of sufficient accuracy to guide a missile.

The zone command node is tasked with monitoring the communications between the emitters, and determining the nature of the threat. The zone command center decides if the aircraft should be fired upon, and tasks one or more battalions to engage the target. The

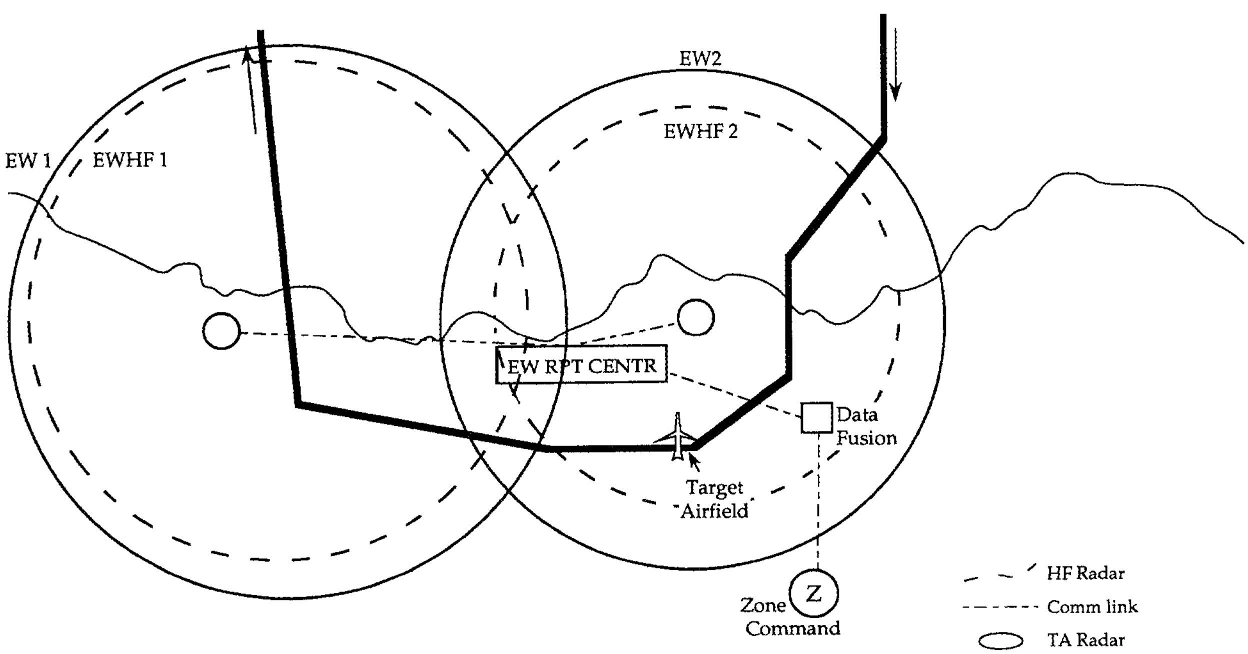

Figure 1. Early warning system.

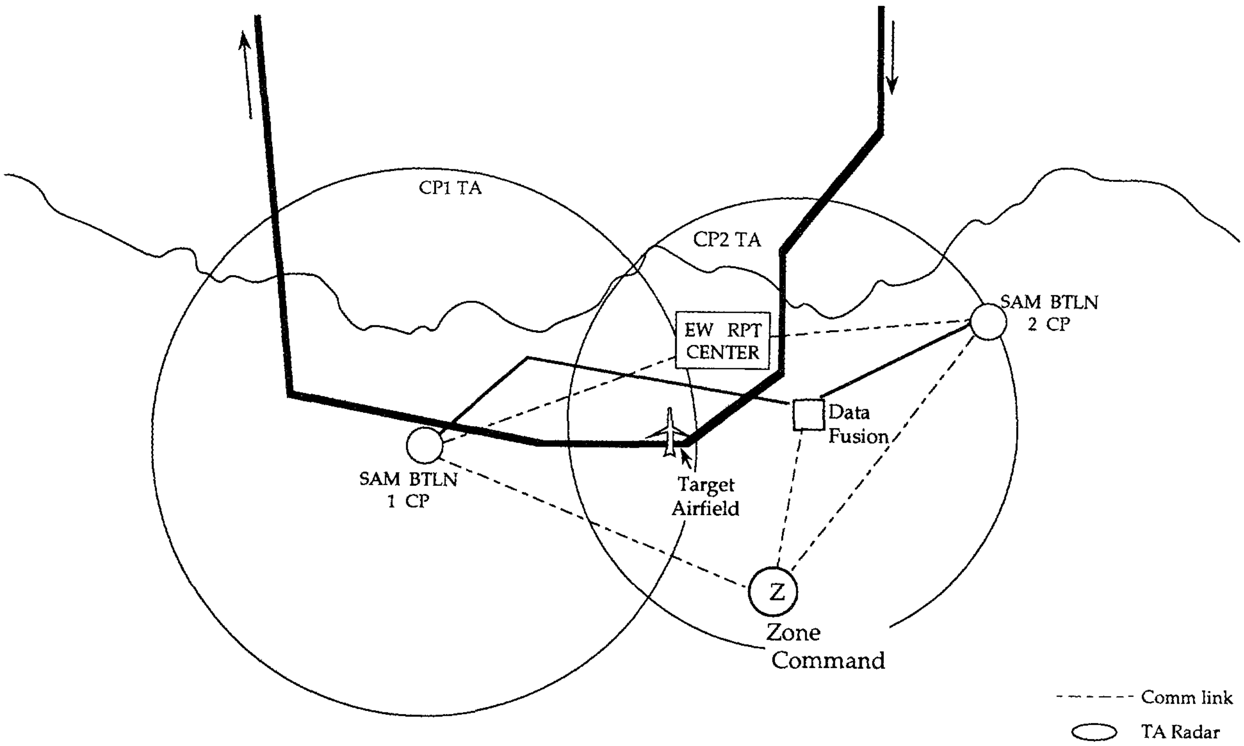

Figure 2. Battalion level target acquisition radars.

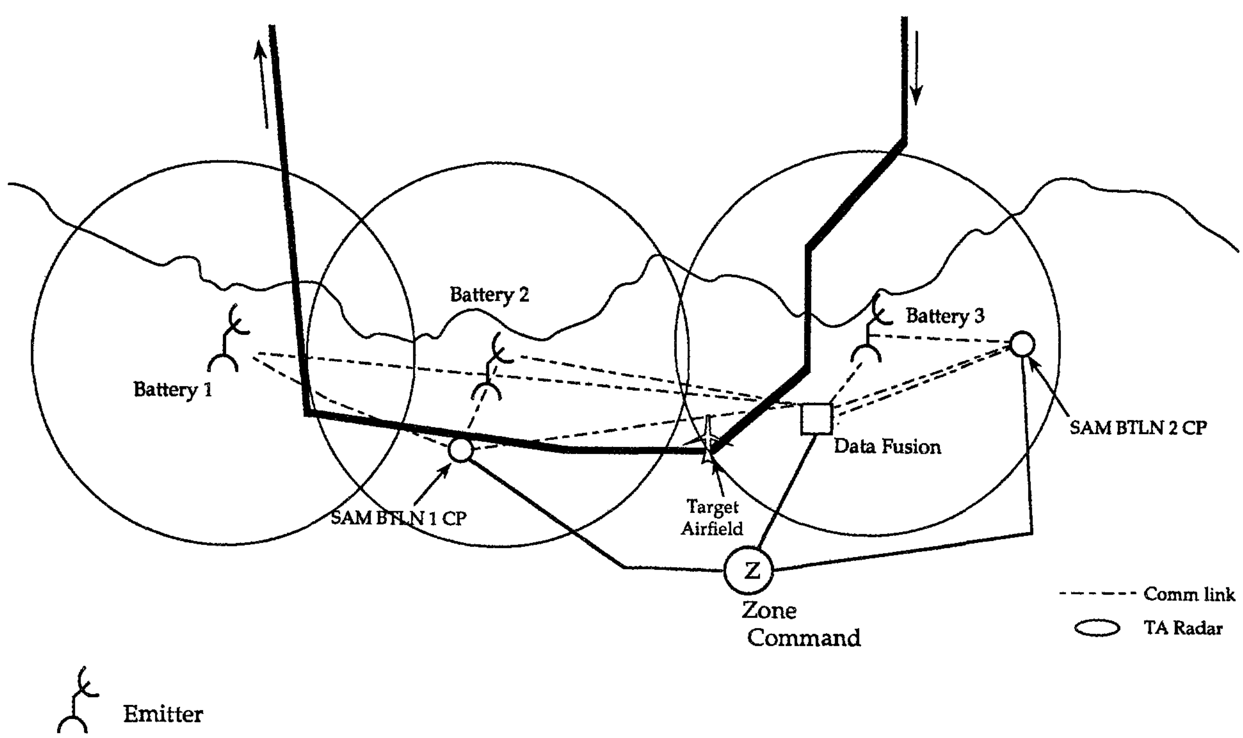

Figure 3. Battery level target acquisition radars.

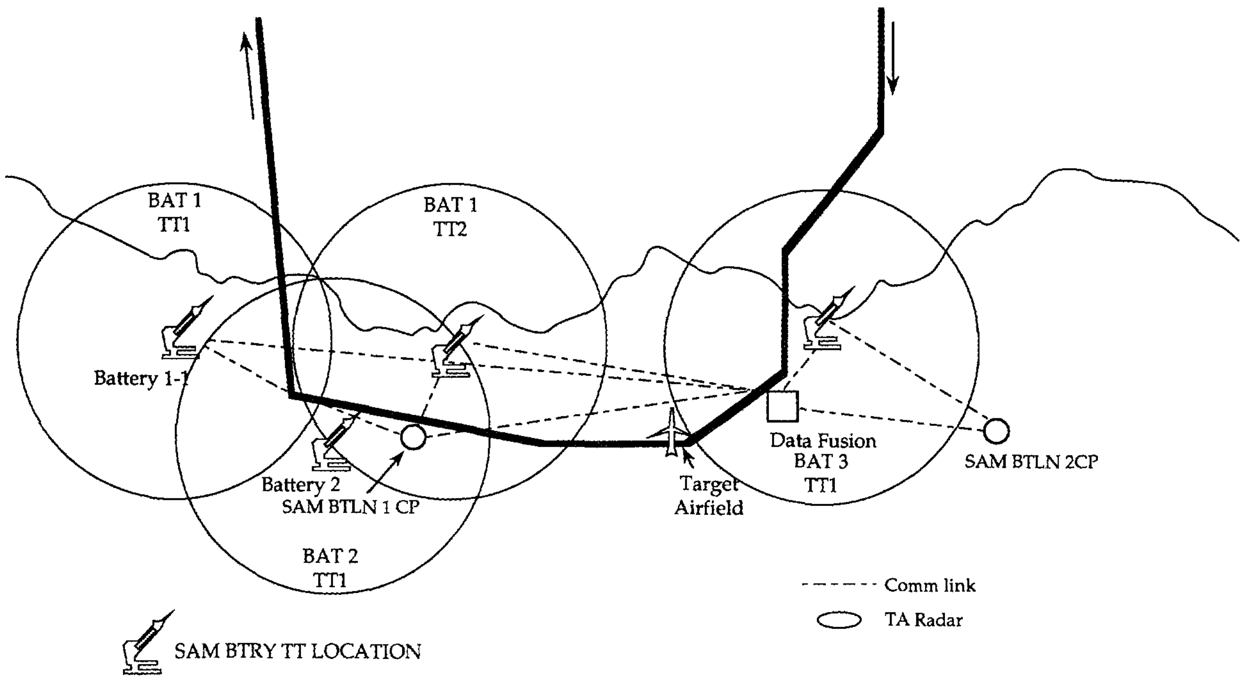

Figure 4. Target tracker radars.

battalion command center receives directives from the zone command center, and tasks its assets to engage the target. In particular, no target tracker can attempt to detect the intruder unless clearance is given by the battalion commander. This is because emissions from a target tracker are considered an act of aggression. The strike group is subject to missile or gunfire whenever a target tracking radar is locked onto the strike group and the battery to which it belongs has been given instructions to engage.

Radar jamming techniques vary in their sophistication and effect. Based on intelligence gathered about the signal characteristics and signal processing of an emitter, as well as the function, designs of ECM equipment are more or less capable of causing combinations of the following effects in radars, communications channels, and data links:

1. slow the detection or transmission task;
2. reduce detection range;
3. prevent a node from receiving transmissions from another node;
4. force two or more emitters to detect the aircraft simultaneously before a track can be established.

Planners of ECM employment use some simple rules of thumb to choose jamming targets and to choose the effect they wish to have on the targeted emitter or link. We will show that, through stochastic network analysis, we can produce performance measures for various trial jamming plans. Furthermore, we can index each emitter's performance in terms of its contribution to the functioning of the overall system. Formally, if T is the (stochastic) performance measure of interest, we will give an algorithm for computing $E[\delta T/\delta V(x)]$, where x is a network activity and $V(x)$ is its (randomly) duration.

The mission of the IADS is to maintain control of the airspace surrounding some high valued target, like the airstrip shown in Figures 1–4. The mission of the strike group is to penetrate this airspace and destroy

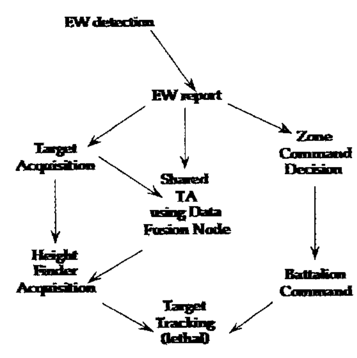

Figure 5. Evolution of an air defense engagement.

the target airstrip. In this work, we will take the perspective of the attacking strike group and the planners of the strike group's ECM.

Our goal as ECM planners is to control the evolution of the IADS's engagement state, preventing the IADS from firing guns and missiles at the strike group. Thus, we will use as our measure of effectiveness the cumulative time that the strike group is subjected to possible missile or gunfire. We will attempt to drive this tracking time to zero by adroitly applying our ECM capabilities. Note that the time of lethal exposure is one among a number of appropriate measures available. The development of the stochastic relaxed Petri net model is not limited to this measure.

We will construct a model that includes a network with random arc lengths to calculate measures of IADS performance. This model will *not* include:

- the effects of penetrator turns;
- autonomous defensive actions;
- airborne interceptor actions;
- damage to the IADS during the engagement;
- the effects of several penetrator axes.

The model we develop here concerns the flow of data and commands through the IADS, as well as providing guidance for the employment of ECM.

2. THE DETERMINISTIC NETWORK

In this section, we construct a class of networks called *relaxed Petri nets*. These networks consist of a directed graph along with some special arc and node designations designed to capture the command structure and data handling mechanisms of an air defense network. It has been observed that this structure is appropriate for modeling in applications as diverse as performance evaluation of multiprocessor computer systems to analysis of the propagation of information in a hierarchical organization.

Let $G = (N, A)$ be a network constructed so that each arc $x \in A$ represents some activity of the IADS. Thus, A will consist of arcs representing emitter detections, decision processes, communications, etc. Let $v: A \rightarrow R^+$ be a nonnegative weight function giving the duration of each activity.

The arc set A is partitioned into two subsets, a set of essential activities E and a set of nonessential activities $E' = A - E$. An essential activity $x \in E$ has the property that no activity $y \in A$ with $\text{tail}(y) = \text{head}(x)$ may commence until activity x is completed. In the PERT fomulation, every activity is essential. For each $n \in N$, the set of essential (nonessential) activities pointing into n is denoted E_n (E'_n).

Among the activities E'_n, we require that k_n of these activities must terminate before any y with $\text{tail}(y) = n$ may commence. We insist that $k_n = 0$ or $k_n < \text{indegree}(n) - |E_n|$. To summarize, an activity $y \in A$ with $\text{tail}(y) = n$ may commence if and only if:

all activities in E_n are complete; (1)

k_n members of E'_n are complete. (2)

These networks are similar to Petri nets, where the places are the nodes, the transitions are the arcs, and the tokens correspond to the assembly of the track and command data. However, our analysis of these structures will focus on their transient response to a threat, rather than their steady-state behavior.

Example 1. Consider the network fragments shown in Figures 6 and 7. There are several conventions for relaxed Petri net diagramming:

1. arcs with stars at their tails represent activities which start at time 0.0;
2. arcs whose tails are small, unlabeled circles represent communications activities;
3. thick circles indicate emitters, while thin circles indicate nonemitting nodes like command posts and data processing centers;
4. dashed arcs represent activities which take zero time units to complete.

For instance, the arc pointing into EW 1 in Figure 6 represents the traversal of the airspace between the

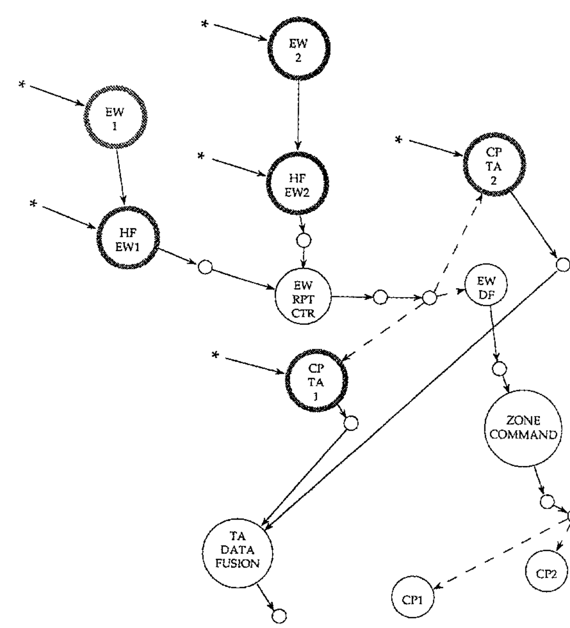

Figure 6. Partial relaxed Petri net, early warning and command portion.

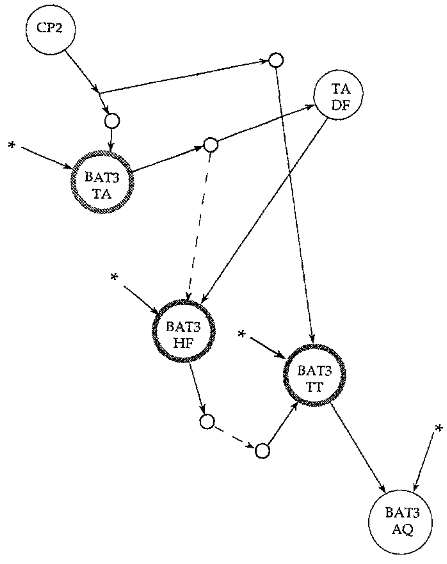

Figure 7. Partial relaxed Petri net, command post 2 and battery 3.

beginning of the scenario and the entry of the aircraft into the detection envelope of early warning emitter 1. Continuing, the arc from EW 1 to HF EW 1 is the EW detection activity, the arc pointing from HF EW 1 to the small, unlabeled circle represents the EW emitter's height finding activity. The arc from the small, unlabeled circle to the EW report center represents the communication of the EW data to the report center.

The report center processes the data (represented by the arc pointing out of EW RPT CTR), and then broadcasts these data to the early warning data fusion (EW DF) node, and to the two command post level target acquisition emitters labeled CP TA 1 (command post target acquisition 1) and CP TA 2. This broadcast takes some time, with the data arriving at each of the recipients at the same time. This is faithfully represented by the arc joining the two unlabeled nodes, and the three dashed arcs pointing to each of the recipient nodes.

Consider the battalion 3 height finder (BAT3 HF) node in Figure 7. It has three arcs pointing into it:

i. the activity that starts at time 0.0 corresponding to the aircraft traversing the airspace between the beginning of the scenario and the maximum detection range of this emitter;
ii. the arc that comes from the target acquisition data fusion (TA DF) node representing the TA DF's communicating TA data from a TA node to this node;
iii. the dashed arc that represents the communication of data from BAT3 TA to BAT3 HF, which takes no time because the TA and HF functions are housed in the same radar system.

The BAT3 HF emitter needs two conditions to be satisfied before its detection task commences. It needs the aircraft to be within its detection envelope, and it needs the two-dimensional track of the aircraft, which is provided by some target acquisition emitter. Thus, arc i is essential, while one of arcs ii and iii must also be completed. Thus, $E_{\text{BAT3 HF}} = \{\text{arc i}\}$, $E'_{\text{BAT3 HF}} = \{\text{arc ii, arc iii}\}$, and $k_{\text{BAT3 HF}} = 1$.

2.1. Measuring Performance of K-Trigger Networks

Let $\{s, t\} \subset N$, $s \neq t$ be network source and sink nodes, respectively. We wish to find the time $T(v)$, which is the maximum of the time that the last member of E_t completes and the time that the k_tth activity in E'_t completes, where v is the aforementioned weight function. This corresponds to the time at which node t has all the input it requires. For instance, let node t represent the issue of firing orders by the command post, $T(v)$ be the time at which all required data are available and (if necessary) permission is granted to fire by higher authorities. To find $T(v)$ we adapt the well known forward sweep algorithm from PERT analysis.

Our algorithm for calculating $T(v)$, which we call algorithm **G**, utilizes some simple notation. States of the algorithm are given by *strings* (ordered sets) of elements in A. If $X_n = x_1x_2 \ldots x_n$ is a string of elements in A, $X_m = x_1x_2 \ldots x_m$, $0 \leq m \leq n$ is called a *prefix* of X_n; this is denoted $X_m \rightarrow X_n$. The symbols $\subset$, $\in$, $\notin$, $\cap$ and $\cup$ will be applied to strings, sets, and combinations thereof, but will always mean the usual operation applied to the underlying sets of the strings. The activity y appended to X_n, $x_1x_2 \ldots x_ny$, is denoted $X_n \cdot y$.

Algorithm G

Initialize: $Y_0 = \emptyset$, $\alpha(Y_0) = \{x \in A\colon \text{tail}(x) = s\}$, $T_0 = 0$, $n = 0$, $\tau(x) = v(x)$ for all $x \in A$

While $\alpha(Y_n) \neq \emptyset$

$n = n + 1$

$y_n = \arg\min_{x \in \alpha(Y_{n-1})} \tau(x)$

$Y_n = Y_{n-1} \cdot y_n$

$T_n = T_{n-1} + \tau(y_n)$

$\tau(x) = \tau(x) - \tau(y_n)$ for all $x \in \alpha(Y_{n-1})$

if $E_{\text{head}(y_n)} \subset Y_n$ and $|E_{\text{head}(y_n)'} \cap Y_n| = k_{\text{head}(y_n)}$, **then**

$$\alpha(Y_n) = \alpha(Y_{n-1}) - \{x \in A: \text{head}(x) = \text{head}(y_n)\} \cup \{x \in A: \text{tail}(x) = \text{head}(y_n)\}$$

$$\alpha(Y_n) = \alpha(Y_n) - \{x \in A: \text{there exists } y \in Y_n \text{ with head}(x) = \text{tail}(y)\}$$

endwhile.

Denote the terminating values of T_n and Y_n by $T(v)$ and $Y_G(v)$, respectively. Let V^+ be the set of nonnegative weight functions on A, $V^+ = \{v: A \to R^+\}$. Let β be the set of strings which may terminate algorithm **G** for weight functions in V^+, $\beta = \{Y_G(v): v \in V^+\}$, and let ζ be a set containing β and all prefixes of elements of β. We will call the sequence $Y_0, Y_1, \ldots, Y_n = Y_G(v)$ the sample path of algorithm **G** for the weight function v. Thus, every possible sample path of algorithm **G** is contained in ζ. Algorithm **G** gets its name from the fact that it is a greedy algorithm on the state-space ζ, where the objective function value of each element of ζ is the length of the longest s-rooted directed path. This observation is presented formally in Bailey (1992).

2.2. Structural Properties of the State Space

We now establish several structural properties of the state-space ζ. These properties become essential when we consider stochastic relaxed Petri nets. Note that each property holds for all nonnegative weight functions $v \in V^+$, so they will hold with probability 1 when $\{V(x): x \in A\}$ is a set of nonnegative random task durations. Let $Y \in \zeta$. Let $j(y) = \min\{i: y \in \alpha(Y_i)\}$ for each $y \in \alpha(Y)$. Let $v \in V^+$ and suppose that $Y_G(v) = y_1 y_2 \ldots y_m$, and $T(v)$ are computed. Let the set $P(v)$ be constructed as

$$y_m \in P(v), \tag{3}$$

$$\text{for every } y \in P(v), \quad y_{j(y)} \in P(v). \tag{4}$$

Lemma 1. *$P(v)$ is a directed (s, t) path.*

Proof. Let $y = y_n$. By definition of $j(y)$, the condition

$$E_{\text{head}(y_{j(y)})} \subset Y_{j(y)}$$

and

$$|E_{\text{head}}(y_{j(y)}) \cap Y_{j(y)}| = K_{\text{head}(y_{j(y)})}$$

is satisfied by appending $y_{j(y)}$ to $Y_{j(y)-1}$. Furthermore, $y \in \alpha(y_{j(y)})$ implies $\text{head}(y_{j(y)}) = \text{tail}(y)$.

By the same logic as given for y_n, we know that $\text{tail}(y) = \text{head}(y_{j(y)})$ for each $y \in P(v)$ with $j(y) > 0$. This backward tracing of the path continues until we have $y_{j(y)} \in \alpha(\varnothing)$ for some $y \in P(v)$. Since $\alpha(\varnothing) = \{y: \text{tail}(y) = s\}$, $y_{j(y)}$ completes the directed (s, t) path.

Lemma 2. $T(v) = \sum_{y \in P(v)} v(y)$.

Proof. Using the indexing of algorithm **G**, we will show that if $y_m \in P(v)$, then

$$T_m - T_{j(y_m)} = v(y_m).$$

Upon accessing $y_{j(y_m)}$, y_m enters $\alpha(Y_{j(y_m)})$ and $\tau(y_{j(y_m)}) = v(y_{j(y_m)})$. On stages

$$j(y_m) + 1, j(y_m) + 2, \ldots, m - 1, \tau(y_m)$$

is decreased sequentially by amounts

$$\tau(y_{j(y_m)+1}), \tau(y_{j(y_m)+2}), \ldots, \tau(y_{m-1}).$$

Note that because of the greediness of algorithm **G**, $\tau(y_m)$ remains nonnegative. At stage $m - 1$, y_m is appended to Y_{m-1} at cost

$$\begin{aligned} T_m - T_{m-1} &= \tau(y_m) \\ &= v(y_m) - [\tau(y_{j(y_m)+1}) + \tau(y_{j(y_m)+2}) + \ldots + \tau(y_{m-1})], \end{aligned}$$

and we have

$$\begin{aligned} T_m - T_j(y_m) &= \tau(y_m) + [\tau(y_{j(y_m)+1}) + \tau(y_{j(y_m)+2}) + \ldots \tau(y_{m-1})] \\ &= v(y_m). \end{aligned}$$

Thus, the summed durations of arcs on the directed (s, t) path given by $P(v)$ determines $T(v)$. Following the terminology of PERT analysis, we call $P(v)$ the *critical path* for the weight function v. It is obvious that $\delta T(v)/\delta v(x) = 1$ for $x \in P(v)$ and $\delta T(v)/\delta v(x) = 0$ for $x \notin P(v)$. Only those jamming assignments made against elements of $P(v)$ affect $T(v)$, jamming noncritical arcs has no affect on the performance of the air defense system.

3. STOCHASTIC RELAXED PETRI NETS

Let $\{V(x): x \in A\}$ be a set of independent nonnegative random activity durations. Let $\{X(t), t \geqslant 0\}$ be a stochastic process with state-space ξ and intertransition times τ_i, $i = 0, 1, 2, \ldots$. Suppose that $X(t)$ has these properties.

Property 1

$P[X(0) = \varnothing] = 1$ and $P[X(t) \in \zeta] = 1$ for $t \geqslant 0$.

Property 2

$$P[X(\tau_{m+1}) = Y_m \cdot x \mid \tau_1, \tau_2, \ldots, \tau_m, X(\tau_m) = Y_m]$$
$$= P[V(x) - (\tau_{j(x)+1} + \tau_{j(x)+2} + \ldots \tau_m) = \tau_{m+1}$$

and

$$V(x) - (\tau_{j(x)+1} + \tau_{j(x)+2} + \ldots + \tau_m)$$
$$\leqslant V(x) - (\tau_{j(z)+1} + \tau p_{j(z)+2} + \ldots + \tau_m)$$
$$\text{for all } z \in \alpha(Y_m) \mid \tau_1, \tau_2, \ldots, \tau_m, X(\tau_m) = Y_m]$$

for all $Y_m \in \zeta - \beta$ and all $x \in \alpha(Y_m)$.

Property 3

$$P[X(t) = Y_m \mid X(t_m) = Y_m] = 1 \quad \text{for all } Y_m \in \beta \text{ and all } t \geqslant 0.$$

Property 1 states that the process always starts in state ∅, the unalerted state. Property 2 states that the transition from state Y_m to $Y_m \cdot x$ is governed by the physical requirements of the system, transition takes place only when activity x is complete and only if no other ongoing activity is not completed sooner. Property 3 provides conditions for absorption of the process in the engagement state of interest.

The following results make explicit the relationship of the process $\{X(t), t \geqslant 0\}$ to sample paths of algorithm **G** for realizations of V. Lemma 3 states that the probability that $X(t)$ passes through the state $Y_m \in \zeta$ at or before time t is equal to the probability that Y_m is a prefix of $Y_G(V)$ and that T_m, the accumulated time of constructing Y_m, is less than or equal to t. Lemma 4 follows immediately, stating that the probability that $X(t)$ is absorbed in $Y \in \beta$ at or before time t is the probability that $Y = Y_G(V)$ and $T(V) \leqslant t$.

Lemma 3. *For $t \geqslant 0$ and $Y_m \in \zeta$,*

$$P[X(t) = Y, Y_m \to Y] = P[T_m \leqslant t, Y_m \to Y_G(V)].$$

Proof. By construction of $X(t)$.

Lemma 4. *For $t \geqslant 0$ and $Y_m \in \beta$,*

$$P[X(t) = Y_m] = P[T_m \leqslant t, Y = Y_G(V)].$$

Proof. Because $Y_m \in \beta$, Y_m is an absorbing state of $X(t)$. Thus, this lemma follows directly from Lemma 4.

Corollary 1. *For $Y \in \beta$,*

$$P[Y_G(V) = Y] = \lim_{t\to\infty} P[X(t) = Y].$$

Corollary 2. *For every $t \geqslant 0$,*

$$P[T_G(V) \leqslant t] = P[X(t) \in \beta] = \sum_{Y \in \beta} P[X(t) = Y].$$

Corollary 1 uses the marginal of $P[X(t) = Y]$ with respect to t to state that the probability that $Y_G(V) = Y$ is the probability that $X(t)$ is absorbed in Y. Corollary 2 states that the distribution of $T(V)$ is the distribution of the absorption time of $X(t)$.

3.1. Exponential Activity Durations

Let $\{V(x), x \in A\}$ be a set of independent, exponentially distributed random variables, $V(x) \sim \exp(\mu(x))$. Exponential activity durations coincide with the assumption that activities complete randomly at a constant rate. For instance, the rate at which a target is acquired by a target tracking radar is constant over time, so long as the state of the network does not change. Modeling activity durations as exponentials has the attractive property that the rate at which a general task is completed, like establishing an EW track, is proportional to the number of EW emitters searching for the strike group. It is feasible to extend this model to the case where rates may vary over time, perhaps as a function of target range or emitter workload.

Let us denote incremental time incurred by accessing x, $\tau(x)$, after m iterations of algorithm **G** as $\tau_m(x)$. Recalling the definition of $j(x)$, note that $\tau_{j(x)+1}(x) = V(x)$.

Lemma 5. *Let $Y_m \in \zeta - \beta$, then for all $x \in \alpha(Y_m)$*

$$P[\tau_{m+1}(x) \leqslant t \mid \tau_1, \tau_2, \ldots, \tau_m, X(\tau_m) = Y_m]$$
$$= 1 - e^{-\mu(x)t}.$$

Furthermore, $\{\tau_{m+1}(x): x \in \alpha(Y_m)\}$ is a set of mutually independent random variables.

Proof. We will induct on m. For $m = 0$, the statement of the lemma reduces to

$$P[\tau_1(x) \leqslant t] = P[V(x) \leqslant t] = 1 - e^{-\mu(x)t}.$$

Now consider that the lemma holds for $m = 0, 1, \ldots, k$. Hence, $\{\tau_{k+1}(x): x \in \alpha(Y_k)\}$ is a set of mutually independent exponential random variables, $\tau_{k+1}(x) \sim \exp(\mu(x))$. Let

$$z = \arg \min_{x \in \alpha(Y_k)} \{\tau_{k+1}(x):$$
$$x \in \alpha(Y_k) \mid \tau_1, \tau_2, \ldots, \tau_k, X(\tau_k) = Y_k\},$$

then by the strong memoryless property of exponential random variables,

$$\{\tau_{k+2}(x) = \tau_{k+1}(x) - \tau_{k+1}(z) \colon x \in \alpha(Y_k) \cap \alpha(Y_{k+1}) \mid \tau_1, \tau_2, \ldots, \tau_k, X(\tau_k) = Y_k, z\}$$

is a set of mutually independent random variables, and

$$\tau_{k+2}(x) = \tau_{k+1}(x) - \tau_{k+1}(z) \sim \exp(\mu(x))$$

for each $x \in \alpha(Y_k) \cap \alpha(Y_{k+1})$. Each $y \in \alpha(Y_{k+1}) - \alpha(Y_k)$ is an activity with tail(y) = head(z), thus $j(y) = k + 1$ and $\tau_{k+2}(y) = V(y)$. Thus,

$$\{\tau_{k+2}(x) = \tau_{k+1}(x) - \tau_{k+1}(z) \colon$$

$$x \in \alpha(Y_{k+1}) \mid \tau_1, \tau_2, \ldots, \tau_k, \ldots, \tau_k, X(\tau_k) = Y_k, z\}$$

is a set of independent exponentials, $\tau_{k+2}(x) \sim \exp(\mu(x))$ for each $x \in \alpha(Y_{k+1})$.

This lemma states that, given the history of the process $X(t)$ until it reaches $Y_m \in \xi$, the incremental time of appending x to Y_m is exponentially distributed and independent of the other elements appendable to Y_m. Thus, the intertransition time of $X(t)$ is the minimum of a set of independent exponentials. For each $Y \in \zeta$, define $\mu(Y)$ as

$$\mu(Y) = \sum_{y \in \alpha(Y)} \mu(y).$$

Define the matrix Q,

$$Q_{X,Y} = \begin{cases} \mu(x) & Y = X \cdot x \in \zeta \\ -\mu(X) & U = X \in \zeta \\ 0 & \text{otherwise} \end{cases}$$

and let $P_{Y,Z}(t) = P[X(t) = Z \mid X(0) = Y]$.

Lemma 6. *For each* $Y \in \beta$,

$$P[T(V) \leq t, Y_G(V) = Y]$$

$$= P[X(t) = Y \mid X(0) = \varnothing] = P_{\varnothing,Y}(t).$$

Proof. This is evident from Lemma 5 and the definition of algorithm **G**.

Note that the generator matrix Q is uppertriangular, so that the Kolmogorov equation $P'(t) = QP(t)$ may be solved sequentially, starting with the boundary conditions $P_{Y,Y}(0) = 1$ for all $Y \in \zeta$, $P_{X,Y}(0) = 0$ for $X \neq Y$. Procedures that solve the Kolmogorov equation numerically include process uniformization; see Ross (1983). Because of the sparse uppertriangular structure of Q significant improvements in standard uniformization are achievable and were implemented to solve the examples presented here.

Corollary 3. *Suppose that we aggregate all basic states into a single absorbing state called* Ψ, *then*

$$P[X(t) = \Psi] = P[T(V) \leq t].$$

Thus, we can calculate the distribution of the time until absorption using the modified process. This distribution is the distribution of the time until the first missile is launched or the first gun is fired.

As stated in Lemmas 1 and 2, if we know $Y_G(v)$ for the deterministic weight function v, we can establish a critical path $P(v)$, such that the partial derivative of $T(v)$ is unity for arcs on the critical path and zero if not. In treating the randomly weighted network, we use the expected value of this partial derivative,

$$C_x = E[\partial T(V)/\partial V(x)]$$

$$= P[x \text{ is on the critical path for } Y_G(V)].$$

In Corollary 4, we establish this quantity and show how it may be computed.

Corollary 4. *For all* $x \in A$,

$$c_x = \sum_{Y \in \beta : x \text{ is critical in } Y} P[Y = Y_G(V)].$$

Computation of criticality indices depends only on the embedded Markov chain of $X(t)$. Experience in real IADS problems has shown that these methods are insensitive to the assumption of exponentiality so long as the embedded Markov chain is correct. Because planners of ECM employment can expect a one-for-one return in the measure of effectiveness for delays in critical activities, the set of probabilities $\{C_x \colon x \in A\}$ serves as indications as to which activities should be attacked by jamming. This idea has some limitations because jamming assignment decisions are discrete, not continuous. However, as we shall see in the next section, critically indices provide new hope for the development of optimal jammer assignments.

4. DELAYED K-TRIGGER NETWORKS

The model presented thus far has an outstanding drawback: some of the activity durations should not be exponentially distributed in length, they should be deterministically known. These are, of course, those activities representing the penetration epoch for each detection envelope. For a known flight route, these times are known with relative certainty and should not be modeled using exponentials. In this section, we remedy this shortcoming. We then present a complete example which illustrates the usefulness of the model in analyzing air defense network performance.

Consider the following modification of the relaxed Petri net with generally distributed activity durations. Suppose that a subset of $\{x: \text{tail}(x) = s\}$ has deterministic duration. Let this set of activities be denoted $D = \{d_1, d_2, \ldots, d_k\}$, where $V(d_i) \leq V(d_j)$ if and only if $i \leq j$. Let $\{\gamma_0, \gamma_1, \ldots, \gamma_k\}$ be a set of probability $|\zeta|$-vectors for each $i = 0, 1, \ldots, k$,

$$\gamma_{i,Y} = P[X(V(d_i)) = Y]$$

with $\gamma_{0,\varnothing} = 1$. At time $V(d_i)$, activity d_i completes and is appended to the current state, so

$$P[X(V(d_i)) = Y \cdot d_i] = \gamma_{i,Y}.$$

We can consider $\{X(t), V(d_i) \leq t \leq V(d_{i+1})\}$ as satisfying Properties 1–3 of Section 3, and having "jumps" at times $V(d_1), V(d_2), \ldots, V(d_k)$.

4.1. An Air Defense Example

Refer back to Figures 6 and 7, the relaxed Petri net fragments corresponding to the situation displays in Figures 1–4. The arcs with starred tails represent activities that begin at time zero. The durations of these activities are flight times from the beginning of the scenario to the penetration of the indicated emitter detection envelopes. We assume that the flight path of the aircraft is fixed, and the velocity of the aircraft is deterministic. Thus, each of these activities is of deterministic duration. By placing these envelope penetration times in increasing order, we get our jump times $\{V(d_1), V(d_2), \ldots, V(d_k)\}$.

We evaluated the network described in Figures 1–4, 6 and 7. The generic times of execution of each type of activity are given in Table I.

After experimenting with some jamming plans commonly used by ECM planners, we created effects 2–7 described in Table II.

The results of jammer asset allocations 2–7 are shown in Figure 8 as boxplots of the time the aircraft is tracked by a target tracking radar. The x symbols represent the 0.025 and 0.925 quantiles of the distribution represented. The box contains the interquantile range of the distribution, while the circle is centered on the median. The upshot of Figure 8 is that, according to our model, none of the jammer asset allocations used in isolation provides a great deal of effectiveness.

Thus, we experimented with combinations of jamming tactics. To guide our search for good combinations, we used the criticality indices for the different emitters in a steepest descentlike heuristic. Note that we do not propose using criticality indices to determine optimal descent directions in an optimization scheme for the following two reasons:

- the decision variables are jam/no jam for each emitter, i.e., this is a discrete optimization problem;
- criticality indices do not account for the role of k_n for node n, and this parameter may be under the control of the ECM planner.

Following the values of the criticality indices and our instincts, we developed jammer allocations 8–11 of

Table I
Expected Activity Durations

Function	Expected Duration (Minutes)
EW detection	1.5
HF detection	0.5
TT detection	1.0
Decision processes	0.5 and 1.0
Communication activities	0.1

Table II
Jamming Asset Allocations

1. Baseline
2. Slowing detections of EW2 and CPTA2 by 100%, reducing corresponding detection ranges 50%
3. Slowing detections of all EWs by 100%, reducing corresponding detection ranges by 50%
4. Force k_{TADF} from 1 to 2
5. Slowing communications to zone command node by 1,000%
6. Slowing all battalion level TA emitters by 100%
7. Remove TA DF capability
8. Plan 7 plus slowing BAT2 TA by 150%, reducing its detection range by 50%
9. Plan 8, plus forcing $k_{\text{ERRPTCTRE}}$ from 1 to 2
10. Plan 9 plus slowing BAT1 HF by 150%, reducing its range by 50%
11. Plan 10 plus slowing BAT1 TA by 150%, reducing its range by 50%

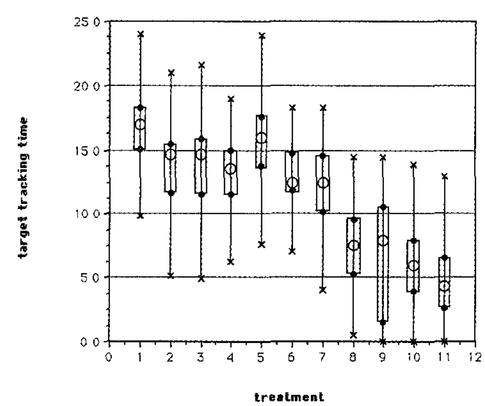

Figure 8. Box plots.

Table II. The changes in criticality of the emitters and decision processes are shown in Figures 9–12. Figure 13 shows the density functions for the duration of time that the aircraft is locked on by a target tracking emitter for each allocation. As expected, the tracking time decreases as we commit more jamming assets.

From Figures 8 and 14, we witness an interesting phenomenon. Although we are able to reduce the critical values of the densities by adding jamming assets, the high percentiles do not decrease significantly. Thus, an airwing commander of extremely conservative mindset might not see any benefit to jamming the radar systems as we have described. Contrastingly, Figure 14 shows the probability of escaping the threat area without being tracked at all. The first jammer asset allocations provide no response at all in this measure. However, the accumulated effect of the different jamming tactics in allocations 8–11 shows dramatic increases in the probability of escaping without target tracker lock-on.

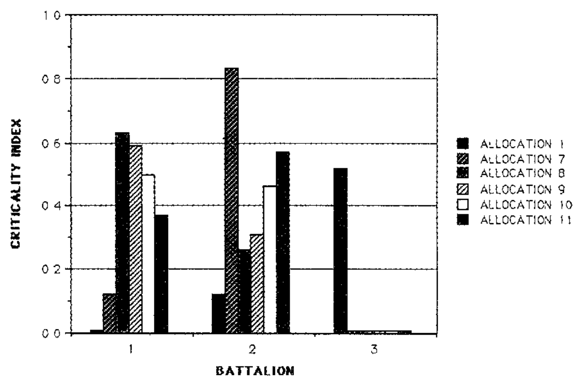

Figure 9. Target acquisition emitter criticality.

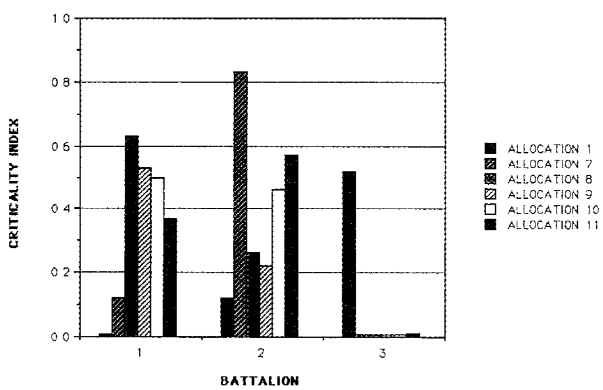

Figure 10. Target finder emitter criticality.

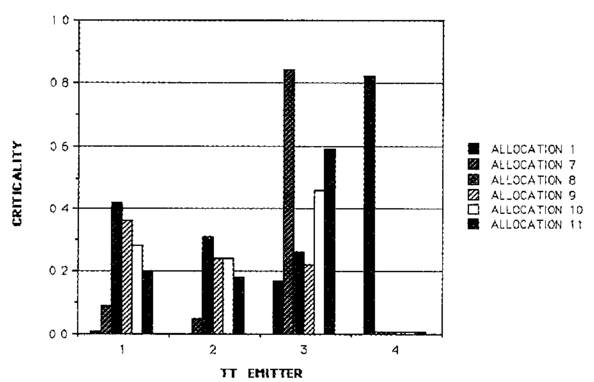

Figure 11. Target tracker criticality.

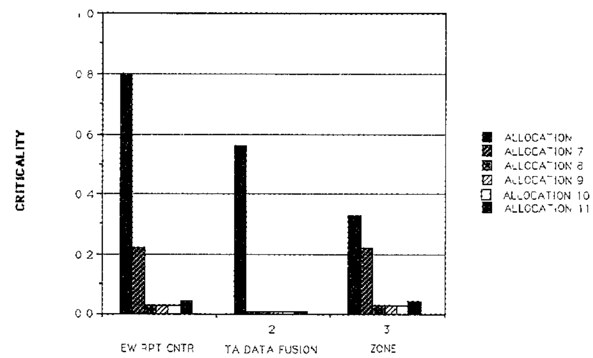

Figure 12. Decision process criticality.

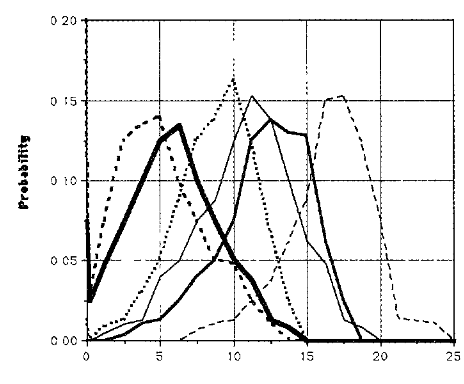

Figure 13. Probability density function for jammer allocations 1 and 7–11. Allocation 1 has the largest mode, while allocation 11 has the smallest. The mode of the density decreases as the allocation number increases.

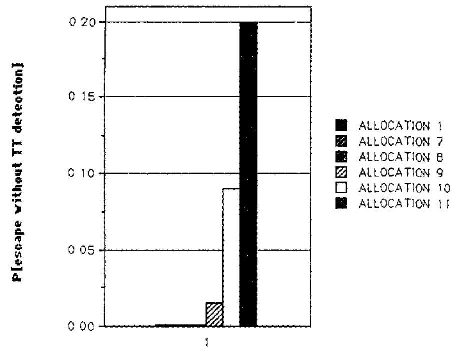

Figure 14. The probability of escaping the threat area without being tracked at all.

4.2. Sensitivity to the Assumption of Exponential Detection and Transmission Times

Our assumption that detection and transmission times are independent, exponential random variables is somewhat restrictive. As we have argued, radar detection of an incoming strike group is plausibly memoryless. The number of scans performed prior to detection is, in physical reality, a geometric random variable, a discrete memoryless random variable. Hence, because interscan times are minute compared to the scale of an air battle timeline, the continuous memoryless distribution, the exponential, is a reasonable model.

We argue that our theoretical development remains valid even when exponentiality is clearly not appropriate. Two results support this premise, one is asymptotic in nature, and the other involves recent developments in the approximation theory of probability distributions.

Suppose that we have radars attempting to perform the same detection task. Each radar has detection time distribution F. Thus, the probability that the time required for the first detection is less than $t > 0$ is given by

$$P[\text{detection before } t] = 1 - (1 - F(t))^n.$$

But, as n gets large, or equivalently, as the threat environment becomes dense, we have

$$1 - (1 - F(t))^n \rightarrow 1 - e^{-f(0)t/n},$$

as n gets large, where $f(0)$ is the value of the associated density of F evaluated at $t = 0$ (see Feller 1970). Thus, as the threat radar environment becomes dense, the time until transition in the stochastic Petri net model becomes approximately exponential regardless of the underlying distribution of the task times. Woodward (1980) builds his description of information theory on the logarithmic message content contained in a small packet of data. Thus, sending messages of deterministic content should require an approximately exponential amount of time.

The second supporting argument involves the work of Johnson and Taaffe (1988a). It has been known for some time that any unimodal distribution having support on $[0, \infty]$ may be approximated by a phase-type distribution (see Neuts 1981). More recent work by Johnson and Taaffe shows methods for performing this approximation for an arbitrary conforming distribution function. Results presented by Johnson and Taaffe (1988b) show these approximations to be quite good in a majority of cases when the context is single server queues.

It is apparent that, without any modifications to the theoretical development or the computational techniques employed, the model described in Sections 3 and 4 of this paper carries through using phase-type distributions.

Because the calculations of criticality indices depend only on the transfusion probabilities of the processes embedded Markov chain, any generalization with an embedded Markov chain does not affect this part of our analysis. For example, one could generalize the system to the semi-Markov case, where transitions and sojourn time are not independent. In this case, the computation of criticality indices does not change. However, computing distributional results becomes very difficult in the semi-Markov model. The moments of the performance measure are accessible through the processes generating function.

Finally, we consider some limited dependency cases. Kulkarni and Adlakha note that arcs emanating from the same node may be dependent, with exponential marginal distributions. They argue that the Markov process method of analysis applies to this case without modification. Since the mechanisms of transition of the stochastic relaxed Petri net we describe are so similar, we feel free to make the same extension without proof. Thus, we may span the spectrum of dependence with our model. Independent activity durations are modeled in Section 4, and completely dependent durations are modeled using combinations of arcs with zero duration in the company of exponentially long activities.

ACKNOWLEDGMENT

This research was sponsored by the U.S. Naval Postgraduate School Research Foundation.

REFERENCES

BAILEY, M. P. 1992. Stochastic Constant Access Systems. *Opns. Res.* **40,** S195–S209.

FELLER, W. 1970. *An Introduction to Probability Theory and Its Applications,* Vol. II. John Wiley, New York.

HAAS, P. J., AND G. S. SHEDLER. 1988. Stochastic Petri Nets With Timed and Immediate Transitions. IBM Almaden Research Center, San Jose, Calif.

HEILENDAY, F. 1988. *Principles of Air Defense and Air Vehicle Penetration.* CEE Press Books, Washington, D.C.

JOHNSON, M. A., AND M. R. TAAFFE. 1988a. Matching Moments With a Class of Phase Distributions: Mixtures of Erlang Distributions of Common Order. Research Memorandum No. 88-10, School of Industrial Engineering, Purdue University, W. Lafayette, Ind.

JOHNSON, M. A., AND M. R. TAAFFE. 1988b. Error Bounds for Queueing-Performance-Measure Approximations Based on Moment Matching, Research Memorandum No. 88-22, School of Industrial Engineering, Purdue University, W. Lafayette, Ind.

KULKARNI, V. G. 1984. Shortest Paths in Networks With Exponentially Distributed Arc Lengths. *Networks* **16,** 255–274.

KULKARNI, V. G., AND V. G. ADLAKHA. 1984. Markov and Markov Regenerative PERT Networks. *Opns. Res.* **34,** 769–781.

LEVIS, A. H. 1986. Modeling and Measuring Effectiveness of C3 Systems. LIDS/P/1608, Laboratory for Information and Decision Systems, MIT, Cambridge, Mass.

NEUTS, M. F. 1981. *Matrix Geometric Solutions in Stochastic Models.* Johns Hopkins University Press, Baltimore, Md.

REMY, P. A. 1986. On the Generalization of Organizational Architectures Using Petri Nets. LIDS/TH/1630, Laboratory for Information and Decision Systems, Massachusetts Institute of Technology, Cambridge, Mass.

ROSS, S. M. 1983. *Stochastic Processes.* Holden Day, New York.

WOODWARD, P. M. 1980. *Probability and Information Theory With Applications to Radar.* Artech House, Dedham, Mass.